

*Citation for published version:*

Sypabekova, M, Jolly, P, Estrela, P & Kanayeva, D 2019, 'Electrochemical Aptasensor using Optimized Surface Chemistry for the Detection of Mycobacterium tuberculosis Secreted Protein MPT64 in Human Serum', *Biosensors and Bioelectronics*, vol. 123, pp. 141-151. <https://doi.org/10.1016/j.bios.2018.07.053>

*DOI:*

[10.1016/j.bios.2018.07.053](https://doi.org/10.1016/j.bios.2018.07.053)

*Publication date:*

2019

*Document Version*

Peer reviewed version

[Link to publication](#)

*Publisher Rights*

CC BY-NC-ND

**University of Bath**

**Alternative formats**

If you require this document in an alternative format, please contact:  
[openaccess@bath.ac.uk](mailto:openaccess@bath.ac.uk)

**General rights**

Copyright and moral rights for the publications made accessible in the public portal are retained by the authors and/or other copyright owners and it is a condition of accessing publications that users recognise and abide by the legal requirements associated with these rights.

**Take down policy**

If you believe that this document breaches copyright please contact us providing details, and we will remove access to the work immediately and investigate your claim.

**Electrochemical Aptasensor using Optimized Surface Chemistry for the Detection of  
*Mycobacterium tuberculosis* Secreted Protein MPT64 in Human Serum**

Marzhan Sypabekova <sup>a, b, d</sup>, Pawan Jolly <sup>c, e</sup>, Pedro Estrela <sup>c\*</sup>, Damira Kanayeva <sup>d\*</sup>

<sup>a</sup> Graduate Program in Science, Engineering, and Technology, School of Engineering, Nazarbayev University, Astana 010000, Kazakhstan

<sup>b</sup> National Laboratory Astana, Nazarbayev University, Astana 010000, Kazakhstan

<sup>c</sup> Centre for Biosensors, Bioelectronics and Biodevices (C3Bio) and Department of Electronic & Electrical Engineering, University of Bath, Claverton Down, Bath BA2 7AY, United Kingdom

<sup>d</sup> Department of Biology, School of Science and Technology, Nazarbayev University, Astana 010000, Kazakhstan

**Present Addresses**

<sup>e</sup> Pawan Jolly has moved to Wyss Institute for Biologically Inspired Engineering, Harvard University, Boston, MA 02115, United States

**Corresponding Authors**

\*(P.E.) E-mail: [P.Estrela@bath.ac.uk](mailto:P.Estrela@bath.ac.uk)

\*(D.K.) E-mail: [dkanayeva@nu.edu.kz](mailto:dkanayeva@nu.edu.kz)

## ABSTRACT

Tuberculosis (TB) remains one of the leading causes of mortality worldwide. There is a great need for the development of diagnostic tests, which are reliable, sensitive, stable, and low cost to enable early diagnosis of TB in communities with scarce resources. This study reports the optimization and evaluation of a synthetic receptor, an aptamer, for the detection of the secreted protein MPT64, which is a highly immunogenic polypeptide of *Mycobacterium tuberculosis*, a causative agent of TB. The study investigates combinatorial effects of an aptamer linker and a co-adsorbent onto a gold electrode for optimal binding efficiency and reduced non-specific interactions for label-free detection of MPT64 using electrochemical impedance spectroscopy. Two types of co-adsorbents and two types of aptamer linkers were studied and high specificity and sensitivity to MPT64 was observed for a surface prepared with a thiol PEGylated aptamer HS-(CH<sub>2</sub>)<sub>6</sub>-OP(O)<sub>2</sub>O-(CH<sub>2</sub>CH<sub>2</sub>O)<sub>6</sub>-TTTTT-aptamer and 6-mercaptohexanol in a ratio of 1:100. The developed aptamer-based sensor was successfully used with spiked human serum sample with a limit of detection of 81 pM. This work demonstrates the use of the MPT64 aptamer as a lower cost, more sustainable and stable alternative of antibodies for the development of point-of-care TB biosensors decreasing the detection time from several days or hours to thirty minutes.

## KEYWORDS

*Mycobacterium tuberculosis*; antigen MPT64; aptamer; surface chemistry; detection; electro-chemistry

## 1. Introduction

In 2015 alone, the worldwide tuberculosis (TB) epidemic accounted for 10.4 million new TB cases, of which 480,000 were multidrug resistant TB, with an estimated 1.4 million deaths (WHO, 2016). TB remains one of the top 10 causes of death worldwide. Despite advances in diagnostics, a considerable proportion of the TB cases reported are still clinically diagnosed rather than bacteriologically confirmed (WHO, 2016). TB detection remains a significant healthcare issue in the developing world owing to a number of challenges. First of all, *Mycobacterium tuberculosis* (*Mtb*), a causative agent of TB, is a slow-growing bacterium, which takes 4-8 weeks to grow on a traditional solid medium and 10-14 days even with a rapid liquid culture (Andersen et al., 2000). Secondly, pulmonary TB presents low clinical symptoms early in the disease course, which leads to a delay in seeking professional care. Thirdly, active pulmonary TB may present a low bacillary burden at the early stage, which often leads to low sensitivity for sputum smear microscopy, commonly used in communities with scarce resources. Therefore, there is a need to develop simple, easily scalable, and accurate diagnostics based on a novel biomarker discovery and new diagnostic assays with an emphasis on alternative non-sputum diagnostics targeting blood, urine or breath (Mehaffy et al., 2017).

The MPT64 protein is one of the biomarkers that is significantly highly expressed in individuals with active TB compared to healthy individuals. The protein is essential for mycobacterial survival and persistence in the host cell. *Mtb* has the ability to inhibit the apoptosis of infected macrophages by deactivating the expression of apoptotic cytokines and hence promoting the survival and virulence of the mycobacteria (Kruh-Garcia et al., 2014). Studies showed that exosomes released from infected macrophages contain mycobacterial proteins, including MPT64. It has been predicted that the existence of MPT64 and other TB proteins could be associated with their function during the establishment and maintenance of an intracellular infection. It has also been reported that these TB-protein enriched exosomes were found to be released into the serum, which opens up the window for diagnostics based on biomarker identification in serum exosomes to reveal active TB in patients (Kruh-Garcia et al., 2014). According to the latest multiple reaction monitoring assays, the clinical diagnostic level of MPT64 protein in isolated exosomes from the serum was at a sub-nanomolar (nM) range (Mehaffy et al., 2017).

Current TB diagnosis based on the detection of MPT64 has been used in skin patch tests, immunochromatographic, immunohistochemical, and enzyme linked immunosorbent based assays

(ELISA) (Arora et al., 2015; Bekmurzayeva et al., 2013; Kohli et al., 2014; Tadele et al., 2014). These methods are based on antigen/antibody interactions. Although routinely used, antibodies have certain limitations in their use in diagnostic tests in low resource settings: expensive production, temperature sensitive, easily undergo functional modifications, limited shelf life (less than 6 months), and often there are batch to batch variations. Other detection studies based on reverse transcription polymerase chain reaction (RT-PCR) targeting the MPT64 gene offer great sensitivity and specificity (Pinhata et al., 2015; Tadele et al., 2014). However, they are cumbersome in resource limited settings and require a relatively expensive set of reagents and trained personnel. Hence, there is a need for the development of an alternative detection methodology for TB.

It has been lately demonstrated that aptamers offer great advantages over antibodies in terms of synthesis scale, cost, and ease of modification. In addition, aptamers have unlimited shelf life, uniform activity regardless of batch synthesis, and are functional under a broad range of conditions defined by the user. Hence, they have a potential to find their application in developing aptasensors for TB detection, where they can serve as bio-recognition elements (Jayasena, 1999; Kuwahara, 2014). The combination of aptamers and sensitive detection methods, such as electrochemical impedance spectroscopy (EIS), would allow increasing the accuracy of the detection. EIS has numerous advantages over other detection techniques. The signal in EIS can be recorded within a small change of an analyte binding event based not only on molecular interaction level but also on electron/charge transfer levels. There have only been a few reports on electrochemical detection of MPT64 antigen using different aptamer sequences (Qin et al., 2009) and various complex surface chemistries (Bai et al., 2017; Thakur et al., 2017a; Thakur et al., 2017b), including electropolymerised poly(3,4-ethylenedioxythiophene) doped carbon nanotubes, gold nanoparticles decorated with fullerene-doped polyaniline, and graphene modified iron-oxide chitosan hybrid nanocomposite film deposited on fluorine tin oxide. Table 1 summarizes currently available TB detection methods including methods approved by WHO for routine use in anti-tuberculosis dispensaries and hospitals.

In our previous work, an aptamer against MPT64 with a dissociation equilibrium constant  $K_D$  of 8.92 nM was selected using the SELEX (systematic evolution of ligands through exponential enrichment) technique. The aptamer was also tested for its specificity on clinical sputum samples (Sypabekova et al., 2017). Here, we report the development of an electrochemical impedance aptasensor for the detection of MPT64 in blood serum. We studied in detail the effect of surface

chemistry and aptamer linker molecule type on the sensor performance since the binding performance of an aptamer to the target is highly dependent on the type of linker between aptamer and the surface and also on the co-adsorbent used (Balamurugan et al., 2006). The type of co-adsorbent influences a considerable reduction of non-specific binding while maintaining the integrity of the immobilized biomolecules (Nogues et al., 2012). In this work, surface chemistries using co-adsorbents 6-mercaptohexanol (MCH) and triethylene glycol mono-11-mercaptopundecyl ether (EG) were investigated for their antifouling properties with combination of different aptamer linker types in the form of HS-(CH<sub>2</sub>)<sub>6</sub>-OP(O)<sub>2</sub>O-(CH<sub>2</sub>CH<sub>2</sub>O)<sub>6</sub>-5'-TTTTT-aptamer-3' and HS-(CH<sub>2</sub>)<sub>6</sub>-5'-TTTTT-aptamer-3' (**Fig. 1**). These linkers were termed as 'long linker' and 'short linker' due to the addition of the extra -OP(O)<sub>2</sub>O-(CH<sub>2</sub>CH<sub>2</sub>O)<sub>6</sub>- to the former.

For the optimized EIS aptasensor in this work, the detection time was significantly reduced compared to traditional detection times, such as sputum microscopy and PCR, from several hours and/or days down to 30 min. The surface chemistry used in this study is comparatively simple with minimal cost, and the detection limit lays well within the current clinical detection range for MPT64, which is in the nM range (Mehaffy et al., 2017). The optimized surface chemistry proposed in this study can be further exploited in developing MPT64 aptasensors for TB diagnosis based on biomarker detection.

## 2. Material and methods

### 2.1. Reagents

Thiolated MPT64 aptamers in the form of HS-(CH<sub>2</sub>)<sub>6</sub>-OP(O)<sub>2</sub>O-(CH<sub>2</sub>CH<sub>2</sub>O)<sub>6</sub>-5'-TTTTT-aptamer-3' (24.3 nmol) were synthesized by Eurogentec (Belgium), and HS-(CH<sub>2</sub>)<sub>6</sub>-5'-TTTTT-aptamer-3' (47.4 nmol) were synthesized by Sigma Aldrich (UK). Phosphate buffered saline (PBS, 0.01 M, pH 7.4) tablets, human serum albumin (HSA, lyophilized powder, ≥97%), human serum (from human male AB plasma), trizma base (≥99.0%), hydrochloric acid (HCl, 37%), magnesium chloride (MgCl<sub>2</sub>, powder, <200 μm), sodium chloride (NaCl, ≥99.5%), sulfuric acid (H<sub>2</sub>SO<sub>4</sub>, 1 M), ethylenediaminetetraacetic acid (EDTA, 0.5 M in H<sub>2</sub>O, pH 8), triethylene glycol mono-11-mercaptopundecyl ether (EG), potassium hexacyanoferrate (III), potassium hexacyanoferrate (II) trihydrate, hexaammineruthenium (III) chloride (Ru(NH<sub>3</sub>)<sub>6</sub><sup>3+</sup>, 98%) and 6-mercapto-1-hexanol (MCH) used in the sample preparation were of analytical grade and purchased from Sigma-Aldrich, UK. Isopropanol (propan-2-ol, HPLC grade), absolute ethanol (HPLC grade) were purchased from

Fisher Scientific (UK). Electrode polishing kit was obtained from BASi Inc. (Japan). MPT64 protein (E5-00061, 1 mg) was purchased from EnoGene (China). Prostate specific antigen (PSA, 100 µg) and carcinoembryonic antigen (CEA, 1 mg) were purchased from Calbiochem (Canada) and USBiological (USA), respectively. All aqueous solutions were prepared using 18.2 MΩcm ultra-pure water with a Pyrogard filter (Millipore, UK).

## 2.2. Apparatus

Measurements were recorded using a CompactStat potentiostat (Ivium Technologies, the Netherlands) with Ivium soft Electrochemistry software. A three-electrode cell with a Ag/AgCl reference electrode (BASi, USA) connected via a salt bridge filled with buffer and platinum counter electrode (ALS, Japan) were used for all measurements. The electrochemical impedance spectrum was measured in a buffer containing 2 mM ferro/ferricyanide  $[\text{Fe}(\text{CN})_6]^{3-/4-}$  redox couple (potassium hexacyanoferrate II/III). The frequency range used for the measurement was in the range of 10 kHz to 100 mHz, with a 10 mV a.c. voltage superimposed on a bias d.c. voltage of 0.2 V vs Ag/AgCl, corresponding to the formal potential of the redox couple. All measurements were performed at room temperature inside a Faraday cage. All measurements were carried out in triplicate, and the mean value of replicates, standard deviations and standard errors from the mean were used to report the results.

## 2.3. Electrode surface preparation

Gold disk working electrodes with 2 mm diameter (CH Instruments, TX, USA) were cleaned mechanically and electrochemically. Electrodes were first cleaned by sonication in absolute ethanol for 10 min, then, mechanically polished for 2 min with 1 µm diamond powder and then with 0.05 µm alumina slurry on respective polishing pads. The electrodes were sonicated for 2 min in isopropanol and for 10 min in Milli-Q water after each step. Electrodes were then cleaned electrochemically in 0.5 M H<sub>2</sub>SO<sub>4</sub> by scanning the potential between oxidation and reduction of gold, -0.05 and 1.1 V vs. Ag/AgCl for 50 cycles. The electrodes were then thoroughly rinsed with Milli-Q water and air dried.

## 2.4. Co-adsorbent and DNA immobilization

For the development of the MPT64 aptasensor with a co-adsorbent (either MCH or EG), gold disk working electrodes were incubated for 16 h at 4 °C with a 150 µl mixture of 100 µM of DNA aptamer (either short linker or long linker) and 100 µM of co-adsorbent, mixed in different ratios. This step was important for the controlled aptamer immobilization on the surface via thiol bonds. The combination of the aptamer and a co-adsorbent used in this study is presented in **Fig. 1**. Both MCH and EG were initially diluted in absolute ethanol at 100 mM to make stock solutions and stored at -20 °C. Further dilutions of both MCH and EG were prepared prior to incubation in different measurement buffers: SELEX buffer (50 mM Tris-HCl; 25 mM NaCl; 5 mM MgCl<sub>2</sub>; pH 7.5), 10× diluted SELEX buffer, and PBS buffer (10 mM and/or 1 mM, pH 7.4). All buffer solutions were filtered using a non-pyrogenic sterile polystyrene 500 ml bottle top filter (Corning Incorporated, USA) and adjusted at room temperature before use. Prior to mixing with co-adsorbents, the DNA aptamer was heated for 5 min at 95 °C and slowly cooled down to room temperature. This step was important to linearize the aptamer sequence and slowly allow it to obtain its most favorable conformation. After incubation, the electrodes were rinsed with the measurement buffer to remove any unattached DNA aptamers. A 150 µl of 1 mM of either MCH or EG was applied onto the surface of the electrodes for another 1 h at room temperature to ensure complete thiol coverage of the gold surface and to displace non-specific interactions between the DNA and gold (Jolly et al., 2015; Keighley et al., 2008). After rinsing the electrodes with the measurement buffer, they were placed into the measurement buffer with 2 mM ferro/ferricyanide [Fe(CN)<sub>6</sub>]<sup>3-/4-</sup> redox couple for at least 1 h for surface stabilization until a stable EIS signal was obtained. The stability measurements were performed in the same time interval that were used for incubation with protein to monitor the drift over time or any changes in EIS due to external factors. Once stable Nyquist curves were recorded, proteins were then incubated to monitor binding events. The stability of the signal was an indicator of the fact that the aptamer had a stable conformational change on the electrode surface with no further fluctuations in EIS signal. The stable signal was used as a baseline for subsequent protein concentration measurements.

## 2.5. Detection of MPT64

Detection of the target MPT64 with the electrochemical aptasensor was achieved by incubating the MPT64 protein for 30 min at room temperature on the surface of the electrode that was pre-immobilized with the co-adsorbent and DNA aptamer. For the detection studies, a wide range of



MPT64 concentrations were used from 24 pM up to 200 nM. MPT64 protein was diluted in different measurement buffers: SELEX buffer; 10× diluted SELEX buffer; 10 mM PBS; 1 mM PBS; 1/10 and 1/100 diluted human serum samples in SELEX buffer.

For the specificity studies different concentrations (0.1, 1, and 10 nM) of the non-target proteins HSA, CEA, PSA, and target MPT64 protein diluted in SELEX buffer were incubated for 30 min on the gold electrode surfaces based on a long linker DNA aptamer/MCH surface chemistry at a ratio of 1/100.

#### *2.6. Preparation and measurement of spiked samples with MPT64*

Serum samples were filtered using a 0.2 µm sterile syringe (Corning Inc.) to remove large molecular formations. The serum dilutions (1/100 and 1/10) were made in SELEX buffer. Co-adsorbent and DNA immobilized electrodes were first stabilized in diluted serum for at least 1h until a stable signal was obtained from the EIS measurement. The electrodes were then incubated in diluted serum with a wide range of MPT64 protein concentrations (from 24 pM up to 100 nM) for 30 min at room temperature.

#### *2.7. BioFET measurements*

Biologically-sensitive field-effect transistors (BioFETs) were used to confirm the EIS results. The BioFET measurements were carried out in an extended gate mode by connecting the gold electrodes via a metal wire to the gate of an n-type metal oxide semiconductor field-effect transistor (MOSFET) (Formisano et al., 2016). The MOSFET readings were recorded using an Agilent B1500A Semiconductor Device Analyzer with EasyEXPERT software. The sensor consisted of thin film gold electrodes (Micrux Technologies, Spain) placed in a flow cell. The FET structure was used to transduce the binding events on the gold electrode into a shift in the threshold voltage of the transistor. An Ag wire coated with silver chloride paste (ALS, Japan) served as a reference electrode. Prior to co-adsorbent/aptamer complex immobilization, electrodes were cleaned by sonication in absolute ethanol for 5 min and then in ultrapure water for additional 5 min. The electrode preparation was the same as described in Section 2.4. Different concentrations (0.001, 0.01, 0.1, and 1 nM) of MPT64 were diluted in SELEX buffer and measured using the same conditions as performed for EIS measurements but without the use of redox markers.

## 2.8. Contact angle measurement

An in-house built optical angle setup was used for contact angle measurement after each immobilization and detection steps (Miodek et al., 2015). Due to the inability of the setup to accommodate the measurement electrodes, thermally evaporated gold electrodes were used instead. The electrodes were sonicated in absolute ethanol for 5 min and then in ultrapure water for another 5 min. Electrodes were then exposed to UV/ozone (BioForce Nanosciences ProCleaner, USA) for 30 min. The MCH/aptamer complex was prepared and incubated overnight as described previously. 50 nM of MPT64 was applied onto the pre-treated surface of the electrode for 30 min, and 50 nM HSA served as a control. Electrodes were then rinsed with ultrapure water and dried under a gentle air flux. Electrodes were then placed on the stage and a 5  $\mu$ l drop of ultrapure water was dispensed. The wetting of surface was then captured using a Nikon p520 camera. Contact angle was measured using an on-screen protractor GNU GPL v3 (<http://osprotractor.sourceforge.net/Protractor.html>).

## 2.9. Chronocoulometry

The surface density of DNA aptamer immobilized on the electrode was determined using chronocoulometry (Formisano et al., 2015; Keighley et al., 2008; Steel et al., 1998). The method was used to determine the optimal ratio for MPT64 detection on the electrode surface at different ratios of long linker aptamer/MCH (1/50; 1/100; 1/200; 1/500) required for MPT64 binding. The final thiol concentration was adjusted to 100  $\mu$ M. Electrodes functionalized with DNA aptamer and MCH were first immersed into 10 mM Tris-HCl (pH 7.4) for 1 h. A potential step from -300 to -800 mV versus Hg/Hg<sub>2</sub>SO<sub>4</sub> was applied for 500 ms, and the resulting charge flow was measured. The same electrodes were then immersed into 100  $\mu$ M hexaammineruthenium (III) chloride (Ru(NH<sub>3</sub>)<sub>6</sub><sup>3+</sup>) in 10 mM Tris-HCl (pH 7.4) buffer, and the resulting charge was again measured. The number of aptamer molecules per electrode area was calculated based on the integrated Cottrell equation (Keighley et al., 2008). The DNA surface density was determined from the surface excess of Ru(NH<sub>3</sub>)<sub>6</sub><sup>3+</sup> as  $\Gamma_{\text{DNA}} = \Gamma_0(z/m)N_A$ , where  $\Gamma_{\text{DNA}}$  is the probe surface density (molecules/cm<sup>2</sup>),  $m$  is the number of negatively charged phosphate groups on the probe DNA,  $z$  is the charge on the redox molecule, and  $N_A$  is Avogadro's constant. The number of DNA molecules for each long linker aptamer/MCH ratio was calculated as the mean of three different electrodes based on the integrated Cottrell equation. For the protein binding studies, the Ru(NH<sub>3</sub>)<sub>6</sub><sup>3+</sup> molecules were

removed from the previously used electrodes by incubating and gently shaking the electrodes in 10 mM Tris-HCl with 10 mM EDTA pH 7.4 for 15 min. The electrodes were then rinsed with the measurement buffer and stabilized for at least 1 h in measurement buffer with 2 mM ferro/ferricyanide  $[\text{Fe}(\text{CN})_6]^{3-/4-}$  redox couple followed by the EIS measurements. The electrodes were then immersed in different concentrations of MPT64 protein (0.1, 1, 10 nM) for 30 min followed by rinsing with measurement buffer, which was then ready for a new EIS measurement recording.

## 2.10. Statistical analysis

All statistical analyses were performed using Graphpad Prism 6 (Graphpad Software, Inc), Origin Pro (OriginLab Corporation), and Excel (Microsoft Office Professional Plus 2013).

## 3. Results and discussion

### 3.1. Surface chemistry optimization studies

The type and the length of the aptamer linker and co-adsorbent were shown to be important for the aptasensor development (Balamurugan et al., 2006). **Fig. 1** presents a schematic overview of the sensor surface chemistries applied in this study, which includes three different types based on either DNA aptamer with short or long linker and MCH and EG as a co-adsorbent. Based on published work on antifouling properties of aptamers with the linker and the EG-type co-adsorbent (Nogues et al., 2012), the combination of short linker DNA and EG as a co-adsorbent was not tested in the current study. This combination is likely to hinder or diminish the availability of the short linker aptamer to MPT64 and make the aptamer inaccessible and/or unavailable to the MPT64 target.

We previously reported a study on selection, characterization and application of DNA aptamers for detection of *Mtb* secreted protein MPT64, where aptamers were selected using the SELEX method and tested on clinical sputum samples using enzyme linked oligonucleotide assay (ELONA) with sensitivity and specificity of 91.3% and 90%, respectively (Sypabekova et al., 2017). The total length of the DNA aptamer was 40 nucleotides, which was modified in this study by the addition of the long linker in the form of  $\text{HS}-(\text{CH}_2)_6\text{-OP}(\text{O})_2\text{O}-(\text{CH}_2\text{CH}_2\text{O})_6\text{-TTTTT}$ -aptamer and the shorter linker  $\text{HS}-(\text{CH}_2)_6\text{-TTTTT}$ -aptamer. The linkers and five thymine residues were included to provide spacing between the aptamer and the surface so that it can easily fold and

capture the protein. The long linker was made of additional ethylene oxide ( $\text{CH}_2\text{CH}_2\text{O}$ )<sub>6</sub>, a hydrophilic part of the linker. This group is essential for protruding the aptamer from the monolayer surface and, thereby, avoiding any steric hindrance associated with protein binding. The ethylene oxide also reduces non-specific binding on the electrode surface (Jolly et al., 2016a; Jolly et al., 2016c). Both MCH and EG are simple and common chemicals that have been used as co-adsorbents in surface functionalization and in the detection of molecules.

To determine which surface chemistry would provide better binding to our protein of interest, the BioFET was recorded after incubating the electrode surface with target MPT64. The BioFET allows the immobilization of an aptamer layer onto an extended gate of a MOSFET and enables fast quantification of an electrical charge variation arising from protein binding. With the BioFET technique, very low limits of detection can be obtained and hence can be used for confirmation of the results obtained from EIS. **Fig. 2a** illustrates a typical transfer characteristic (drain current,  $I_D$ , vs. gate-to-source voltage,  $V_{GS}$ ) curve for an electrode before and after MPT64 binding event onto the surface of the functionalized gold electrode. Depending on the surface charges of the protein, the BioFET can produce a positive or negative shift in its transfer characteristic. Any changes in  $V_{GS}$  modulate the threshold voltage of the transistor and thereby alter the drain current (Aliakbarinodehi et al., 2017). Surface charge analysis for MPT64 previously showed that positively charged hydrophilic amino acids, such as arginine and lysine, were found to be grouped on the surface of the protein. Hence, the positive charge of MPT64 produced a negative shift in the  $V_{GS}$  of the BioFET as can be seen in **Fig. 2a**. **Fig. 2b** presents the values of  $\Delta V_{GS}$  for different MPT64 concentrations (0.001, 0.01, 0.1, 1 nM) on different surface modifications onto the IDE gold electrode: i) a short linker aptamer/MCH, ii) a long linker aptamer/EG, and iii) a long linker aptamer/MCH. The  $\Delta V_{GS}$  for all three surface chemistries was determined at  $I_D=22.5 \mu\text{A}$ . The  $\Delta V_{GS}$  for the long linker aptamer/MCH complex increased from -17.35 mV to -42.13 mV when the MPT64 concentration increased from 1 pM to 1 nM. The combination of the two other surface chemistries (long linker DNA aptamer/EG and short linker DNA aptamer/MCH) studies showed inconsistent changes in  $\Delta V_{GS}$  (**Fig. 2b**) with large error bars. This inconsistency could be due to non-specific binding of the target protein to the functionalized surface and reduced reproducibility. The BioFET data suggests that the surface chemistry based on the long linker DNA aptamer/MCH (**Fig. 1c**) would provide better antifouling properties for MPT64 binding, better reproducibility, as well as improved specificity towards the protein detection.

We also recorded the EIS signal for the three surface chemistries: short linker DNA aptamer/MCH, long linker DNA aptamer/MCH, and long linker DNA aptamer/EG. The surface chemistry based on a short linker-DNA aptamer/MCH (**Fig. 1a**) showed a concentration dependent increase in charge transfer resistance  $R_{ct}$  change (3.9%, 7.5%, and 13.3% at 0.1, 1, and 10 nM of MPT64, respectively) (see Supplementary Information, **Fig. S1**). The same surface chemistry showed a non-specific interaction with HSA (with a  $R_{ct}$  change between 2.3% at 0.1 nM and 12.3% at 10 nM). The results for this specific surface chemistry showed that the short linker aptamer/MCH approach, although sensitive to MPT64, it does not prevent the binding of interferent molecules, hence making it an unreliable surface for use with complex samples. In addition, the large error bars in **Fig. S1** (Supplementary Information) are indicative of electrode to electrode variability. The surface chemistry based on the long linker DNA aptamer/MCH (**Fig. 1c**), measured with redox markers in solution, showed a  $R_{ct}$  signal change that increases with MPT64 concentration (5.8%, 12.0%, and 21.2% for 0.1, 1, and 10 nM of MPT64, respectively), whereas it remained almost unchanged (less than 4%) when incubated with HSA up to a concentration of 10 nM (Supplementary Information, **Fig. S1**). These measurements were recorded upon a 1/100 ratio of long linker DNA aptamer/MCH. This significant increase in  $R_{ct}$  signal from 5.8% up to 21.2% for MPT64 compared to other surface chemistries studies could be due to the blocking effect to electron transfer after attachment of protein onto the surface of the modified electrode. Another reason could be due to the extended nature of the aptamer that forms a brush like conformation, which protrudes from the short MCH monolayer (Nogues et al., 2012). Thereby, the freely moving extended nature of the aptamer with the long linker enabled MPT64 to bind more efficiently compared to other surface chemistry studies and reduced a non-specific binding. The long linker-DNA aptamer/EG based surface chemistry (**Fig. 1b**) promotes the formation of an insulating surface, not suitable for Faradaic measurements. Therefore, measurements were conducted without the use of the redox probes (i.e. in a non-Faradaic mode) to evaluate the capacitive processes on the surface. A complex capacitance was calculated and used in order to evaluate the capacitance from the impedance data (Keighley et al., 2008). The signal at the beginning of the recording was quite unstable and no significant changes were observed in the capacitance upon MPT64 binding (Supplementary Information, **Fig. S2**). Aptamers with longer linker type previously exhibited a 4-fold increase in binding capacity compared to those with shorter linkers (Balamurugan et al., 2006). Therefore, the surface chemistry based on the long linker DNA aptamer/EG did not show any

sensitivity towards MPT64 nor specificity (data not shown); hence, it was concluded not to use this surface chemistry for further MPT64 detection. As the result of both BioFET and EIS measurements, the surface chemistry based on the long linker DNA aptamer/MCH was chosen for further analysis.

### 3.2. Contact angle measurement

The contact angle measurement was used to validate each functionalization step in the aptasensor development and to demonstrate the binding between the target and modified surface. The contact angle was determined at different stages of the aptasensor development. **Fig. S5** presents the obtained results (see Supplementary Information; the contact angle images are shown in **Fig. S6**). The surface of the electrode was hydrophilic for all measurements because of UV/ozone exposure during electrode surface preparation and cleaning steps. The contact angle of the bare gold electrode was  $16.3^\circ$  and an increase to  $21.2^\circ$  was observed after the MCH functionalization step. The contact angle value for the aptamer/MCH at 1/100 ratio was lower ( $20.5^\circ$ ) compared to MCH alone indicating on a successful immobilization of aptamers on the surface. The subsequent interaction with 50 nM MPT64 target significantly lowered the value of the contact angle down to  $16.5^\circ$ , demonstrating a specific binding to immobilized aptamers compared to control protein, HSA ( $19.7^\circ$ ). A small non-specific binding of HSA to the MCH treated surface was also shown in previous studies (Balamurugan et al., 2006; Jolly et al., 2015; Jolly et al., 2016b). However, the change for non-specific binding was much lower than for specific binding and could be attributed to noise.

### 3.3. Long linker DNA aptamer/MCH ratio optimization

The aptamer surface density on the gold electrode and aptamer geometry/positioning is extremely important for consequent target binding. Therefore, finding the best ratio of an aptamer and a co-adsorbent is essential for the aptasensor functionalization and development. Since the long linker aptamer/MCH complex based surface chemistry showed the highest signals in BioFET and EIS measurements, it was used further in the optimization analysis. A chronocoulometric method was used to determine the surface density of DNA aptamer (Keighley et al., 2008) so that the optimal aptamer/MCH ratio is obtained for maximum signal upon MPT64 binding. The method was based on the electrostatic interaction or intercalation of specific redox cations ( $\text{Ru}(\text{NH}_3)_6^{3+}$ ) with the DNA's sugar-phosphate backbone. The amount of trapped redox marker at the DNA-

modified electrode then determined using chronocoulometry. The surface density of the probe was calculated assuming complete charge compensation of the DNA phosphate residues by redox cations (Steel et al., 1998). The long linker DNA aptamer was co-immobilized with MCH onto the gold electrode, where the probe surface density was controlled by varying ratios of DNA aptamer and MCH in solution. A typical charge flow graph (Supplementary Information, **Fig. S3a**) and chronocoulometric response curve (Supplementary Information, **Fig. S3b**) with and without  $\text{Ru}(\text{NH}_3)_6^{3+}$  for the long linker DNA aptamer/MCH at 1/100 ratio showed the difference in charge flow. The data from the graphs was used to determine the DNA aptamer density using the integrated Cottrell's equation (Keighley et al., 2008).

The variation of the surface density of the long linker DNA aptamer at different ratios of MCH is shown in **Fig. 3a**, where four DNA aptamer/MCH ratios were tested: 1/50, 1/100, 1/200, and 1/500. The DNA aptamer density increased as the fraction of DNA to MCH increased from  $6.50 \times 10^{11}$  molecules/cm<sup>2</sup> at 0.002% (1/50 aptamer/MCH) fraction of DNA up to  $7.91 \times 10^{11}$  molecules/cm<sup>2</sup> at 0.02% (1/500 aptamer/MCH) DNA (Table 2). The aptasensor was further tested on target binding at three different MPT64 concentrations (0.1, 1, and 10 nM) by impedance measurements and the results were compared for different aptamer/MCH ratios (**Fig. 3b**). By analyzing the  $R_{ct}$  change responses from the EIS signal, the four aptamer/MCH ratios showed different levels of  $R_{ct}$  change after incubating with MPT64. A significant increase in MPT64 binding was recorded at an aptamer/MCH ratio of 1/100 by the EIS compared to other ratios studied; the  $\Delta R_{ct}$  signal increased in the ratio sequence  $1/500 < 1/50 < 1/200 < 1/100$ . A similar trend was also reported for aptasensors against prostate specific antigen (Formisano et al., 2015). The 1/100 ratio with aptamer  $7.66 \times 10^{11}$  molecules/cm<sup>2</sup> showed the highest  $R_{ct}$  shift: 3.0%, 10.4%, and 24.7% upon MPT64 binding at concentrations 0.1, 1, and 10 nM, respectively. However, the 1/50 ratio showed lower  $R_{ct}$  change (0.01%, 1.6% and 11.6% at 0.1, 1 and 10 nM, respectively) compared to the 1/100 ratio, and it didn't follow the same trend as with the other ratios studied. This might indicate that the surface was too densely packed, which lowered the sensitivity towards the MPT64 at 1/50 ratio due to steric hindrance effects. Taking into consideration the long linker that was attached to the aptamer and the size of the aptamer itself, which was comparatively long (40 nucleotides), the densely packed surface disabled the aptamer from specific binding to the MPT64. This could be due to the fact that aptamer configuration did not have a freely moving brush-like confirmation or it was due to the charge effects from the DNA at 1/50 ratio. Since it is extremely important to find

the balance which gives an optimal signal, a ratio of 1/100 was chosen for further sensor development.

#### 3.4. Concentration dependent analysis and specificity studies

A schematic overview that represents a binding event of the target MPT64 over the pretreated gold surface of the electrode with the long linker DNA aptamer/MCH is depicted in **Fig. 4a**. The typical Nyquist plot in the measurement buffer for an electrode with a bare surface, immobilized with the long linker DNA aptamer/MCH before and after interaction with 50 nM MPT64 for 30 min is presented in **Fig. 4b**. The EIS signal for the aptamer modified electrode was recorded repetitively in 30 min intervals until a stable signal was obtained. This stable signal as used as a baseline and all the protein incubation signals are reported with respect to this baseline. Any signal arising from a possible conformational change of the aptamer in the presence of the measurement solution itself is therefore already included in the baseline.

A concentration dependent curve for different MPT64 concentrations using a long linker DNA aptamer/MCH in a ratio of 1/100 relative to blank measurements from the EIS signal measured in SELEX buffer is presented in **Fig. 4c**. A concentration dependent analysis was performed for MPT64 concentrations ranging from 49 pM to 200 nM and showed an increase in charge transfer resistance ( $R_{ct}$ ) change upon increasing the target concentration. A plateau was reached at 50 nM concentration of the target MPT64 indicating that the surface was saturated above this concentration. A linear correlation was found between  $R_{ct}$  change value and target protein in the range of 1-50 nM. The regression equation for  $R_{ct}$  change versus MPT64 concentration was  $y=0.3395x+11.735$  with  $R^2=0.97$ , where  $x$  is the concentration of MPT64 in nM (**Fig. 4c** inset). **Fig. 4d** presents an experimental and fitted Nyquist plot for binding of MPT64 at concentrations ranging from 49 pM to 50 nM using the long linker DNA aptamer/MCH in a ratio of 1/100. A Randles fitting circuit was used in this study to quantify the target analyte (Liang et al., 2013). **Fig. 4d** inset shows the Randles equivalent circuit model selected to fit the experimental data, in which  $R_s$  is the solution resistance connected in series with a constant phase element  $CPE$  and in parallel with the charge transfer resistance  $R_{ct}$  of the surface and Warburg element  $W$  to model diffusion.

The aptasensor based on the long linker DNA aptamer/MCH surface chemistry (**Fig. 1c**), measured in solution with redox markers, showed a  $R_{ct}$  signal change that increased by 5.82% at 0.1 nM, 12% at 1 nM, and 21.2% when it was incubated with 10 nM MPT64, whereas it remained less



than 4% at the same concentrations (0.1, 1, and 10 nM) for the control proteins HSA, CEA, and PSA showing specificity towards MPT64 (**Fig. 5**). A non-target protein such as CEA (180 kDa) was selected in this study because it is a member of a family of cell surface glycoproteins that are produced in excess in human colon carcinomas (Benchimol et al., 1989) with normal level in healthy individuals being at <5 ng/ml (Asad-Ur-Rahman and Saif, 2016), which is equivalent to 0.02 nM. PSA (30 kDa) is serine protease produced at high concentrations by normal and malignant prostatic epithelium (Stenman et al., 1999) with normal levels in healthy individuals being at 4 ng/ml (Thompson et al., 2004), which is equivalent to 0.13 nM. The maximum concentration used for the specificity study in this work was 10 nM, which is 500 times higher for CEA and 77 times higher for PSA than the normal clinical range. Therefore, the use of higher concentrations for CEA and PSA could account for combinatorial interference effects of these proteins on MPT64 detection as opposed to normal level standards. HSA is the most abundant protein in plasma comprising about half of serum proteins with a molecular weight of 66.5 kDa (He and Carter, 1992) with average concentration being at 35 mg/ml (Doumas et al., 1971). All control proteins were used as a control at the same concentration to confirm that selected aptamers are indeed specific to MPT64. Upon exposing the aptasensor to 10 nM HSA in measurement buffer, an increase in the  $R_{ct}$  value of around 4-5% was recorded (**Fig S1, Fig 5.**). Such an effect could be a blocking effect due to occupancy of free MCH spaces on the sensor surface. The experiments with human serum samples presented in Section 3.6 show that the change upon MPT64 binding is consistent with that found in measurement buffer despite of serum being rich on other proteins, including HSA.

In our previous study on selection, characterization, and application of DNA aptamers for detection of *Mtb* secreted protein MPT64, bioinformatics surface charge analysis (PDB code 2hhi) showed that positively charged hydrophilic amino acids, such as arginine (ARG85 and ARG117) and lysine (LYS118) were grouped on the target MPT64 model, allowing a potential binding site for the negatively charged DNA backbone with common TCCAGT located within the biggest potential stem loop (hairpin), formed by four Watson-Crick base pairs in stem parts and having six bases in loop part (Sypabekova et al., 2017). A computed GC/AT ratio  $(G + C)/(A + T)$  of the selected MPT64 aptamer had about 1.11 that provided basic sequence characteristics in terms of nucleotide composition. This work could provide an understanding of how the target MPT64 and

aptamer bind and a study, such as analysis of crystal structure of the protein/aptamer complex needs to be done to understand the exact mechanism of binding.

### 3.5. Buffer optimization studies

Electrodes functionalized with the long linker-aptamer/MCH at optimized ratio of 1/100 were further used for buffer optimization studies using the EIS technique. These buffers include the measurement buffer (SELEX buffer; pH 7.5) in which the aptamer was initially synthesized (Sypabekova et al., 2017), 10 times diluted SELEX buffer (pH 7.5), 10 mM PBS (pH 7.4), and 1 mM PBS (pH 7.4). The reason for diluting buffers was to reduce the amount of charge screening during the detection and examine whether dilution influenced the binding efficiency. Upon dilution, the pH of buffers was adjusted back to the original value. Preparation of 1/100 aptamer/MCH, stabilization of the electrode surface in the measurement buffer and EIS measurements and rinsing in between steps were carried out as described in Section 2.4 and were all performed in each type of buffer. These buffers were used in rinsing steps, in recording the EIS signal, as well as in diluting the target MPT64. A concentration dependent curve of  $R_{ct}$  change with different concentrations of MPT64 measured in SELEX buffer is presented in Supplementary Information, **Fig. S4a**. The increase in  $R_{ct}$  signal and relatively small error bars for the SELEX buffer was consistent with the increase of protein concentration. When the SELEX buffer was diluted 10 times, the recorded signal change was below zero at lower MPT64 concentrations (from 100 pM to 1 nM) (Supplementary Information, **Fig. S4b**). The reason for such a drop in the recorded signal value could be the result of combination of different processes including the change in aptamer conformation upon binding to MPT64. The magnesium ions within the SELEX buffer are essential for DNA to form a stable structure (Serec et al., 2016); therefore, the decrease in magnesium might have hindered the proper aptamer folding and eventually resulted in screening of negative charges of DNA aptamers resulting in reduced  $R_{ct}$  change. An increase in  $R_{ct}$  was observed with higher MPT64 concentrations (<1 nM) due to the binding event of the protein onto the electrode surface, which disabled the access of the redox probe from the close proximity of the electrode surface. In addition, batch-to-batch variations were observed, which led to having a high standard deviation at each sample point; this could be a result of differences in the initial  $R_{ct}$  values from each electrode at the same protein concentrations. These variations are due to the destabilization of the ap-

tamer/protein complex formation. Consequently, there were significant differential values in overall  $R_{ct}$  change. Next, measurements were performed in PBS buffer, a widely used buffer in the development of aptasensors. A seemingly random change in  $R_{ct}$  at 10 mM PBS (Supplementary Information, **Fig. S4c**) could be explained by the unstable interaction of MPT64 molecules with the electrode surface. We presume that there was the promotion of non-specific and unstable protein-protein interactions. The same scenario was observed with 1 mM PBS; although with decreased  $R_{ct}$  change (<15%) (Supplementary Information, **Fig. S4d**). Clearly, results of this study indicated the importance of the buffer in the development of sensitive and specific aptasensor for the detection of *Mtb* secreted protein MPT64 and showed that the buffer, where aptamers have been previously raised, could give a better and consistent signal response.

### 3.6. Analytical evaluation of the aptasensor using serum samples

The developed aptasensor with optimized surface chemistry was tested on human serum samples using EIS. For the determination of the MPT64 in serum, the established standard curve of the aptamer sensor in buffer solution was not used; rather the standard curve of the aptamer sensor in serum was used. The standard curve for the aptamer sensor in serum was established by stabilizing the electrode surface in serum to have a good calibration signal. The electrode surface was primarily stabilized with 1/100 diluted serum until obtaining a stable signal. There are other molecules such as albumins within the serum that could be absorbed on MCH, hence, the stabilization step is important to have a good calibration signal. The electrochemical impedance signal increased when the aptamer-modified electrode was immersed in serum when compared to the results obtained with the buffer (**Fig.6a**). In serum, which contains high concentrations of HSA as in the normal clinical range, the optimized surface chemistry showed a non-specific binding with  $R_{ct}$  change of around 5-6% without going beyond during repetitive measurement in serum alone (**Fig.6b**, dashed line). This suggests a possible resilience to the non-specific binding of serum proteins.

After a signal stabilization, the electrode was incubated in human serum with a wide range of MPT64 concentrations (from 12 pM to 100 nM) (**Fig. 6b**). There was an increase in  $R_{ct}$  with an addition of the target MPT64 at different concentrations in 1/100 diluted serum samples (**Fig.6**). The sensor demonstrated a clear distinction between specific binding of MPT64 and non-specific binding of HSA not exceeding 6%  $R_{ct}$  change. The signal after stabilization was used as a reference

to calculate the  $R_{ct}$  change during MPT64 detection. A concentration dependent response was obtained with a gradual increase in  $R_{ct}$  signal up to 50 nM MPT64 demonstrating a good response down to concentrations of 49 pM with the limit of detection (LOD) of 81 pM for MPT64 detection (**Fig. 6**). The smallest protein concentration tested was 12 pM. Hence, at concentrations of 12 pM and 24 pM the signal change was negligible. The LOD was calculated using the formula  $LOD = \text{mean}_{\text{blank}} + 1.645(SD_{\text{blank}}) + 1.645(SD_{\text{low concentration sample}})$ , where SD is standard deviation (Armbruster and Pry, 2008; Armbruster et al., 1994). The signal for diluted serum alone remained unchanged throughout the experiment. The surface of the sensor started to saturate at around 50 nM of MPT64, similarly to what was observed with the measurements after incubation in SELEX buffer. The  $R_{ct}$  change gives slightly higher response after incubation with respective concentrations of MPT64 in diluted serum compared to those diluted in SELEX buffer (Supplementary Information, **Fig. S8**). We assume that the composition of serum could promote the formation of MPT64 multimers. MPT64 can form multimeric structures, tetrameric structures to be exact, in isolates with subunits being covalently connected via disulphide bonds (Chu and Yuann, 2011). Therefore, instead of having one MPT64 on the electrode surface it was estimated that tetrameric MPT64 could be attached onto the aptamer modified electrode. A slight increase in  $R_{ct}$  in serum measurements could be as the result of an attachment of MPT64 tetramers to the aptasensor surface. MPT64 forms tetrameric structures and not agglomerates, hence, the attachment of MPT64 tetramers to the aptasensor surface could not form a non-specific adsorption. The strong covalent bond of MPT64 tetramers cannot be removed by sufficient rinsing, unless by adding a detergent (urea or DTT) to an electrode surface. Since the aptamer was attached onto the electrode surface via such S-S bond, the addition of detergent to an electrode surface could detach the aptamer from the electrode surface. The rinsing of the electrode was done sufficiently, and hence, we believe that the interaction between the aptamer and the MPT64 tetramers are specific.

We also performed measurements in less diluted serum (1/10 dilution), which gave a much higher LOD (12.73 nM) (Supplementary Information, **Fig. S7**). Since there was a pool of other proteins and molecular agglomerates present in less diluted serum, the chances for MPT64 multimer to move freely and reach the aptasensor surface was limited thereby giving a lower signal change in the charge transfer resistance. During cellular infection with *Mtb*, mycobacterial products including the MPT64 biomarker incorporates into host cell exosomes, 100 nm vesicles which are then released into the biological fluid (Giri et al., 2010; Mehaffy et al., 2017). The current

clinical diagnostic level of MPT64 protein in isolated exosomes from the serum is at a sub-nanomolar range (Mehaffy et al., 2017). Hence, the detection limit of the current aptasensor is in the range of detecting MPT64 in clinical samples and therefore, it could be further adopted as one of the rapid MPT64 detection methods.

#### 4. Conclusion

In this study, strategies for the optimization of an EIS aptamer based sensor for the detection of *Mtb* secreted antigen MPT64 was investigated. It was concluded that the combination of the long linker aptamer/MCH was optimal for the sensitive detection of MPT64. The aptamer was specific to MPT64 as shown by EIS and contact angle measurement experiments. BioFET results confirmed the importance of the combination of the long linker aptamer/MCH. The aptamer surface density of 1/100 ratio provided the maximum impedimetric signal compared to other ratios studied. The importance of the buffer was also established for MPT64 binding and the SELEX buffer, in which aptamers were synthesized, was found to be the optimal buffer to conduct the measurements. The aptasensor was tested with spiked human serum and evaluated in dose response analysis. The measurements were reproducible with a LOD of 81 pM, which is in the range of detecting MPT64 in clinical samples. The current study showed a significant reduction in detection time compared to traditional detection methods by reducing time from several hours and/or days to 30 min. Moreover, the aptasensor in this study used a relatively simple surface chemistry based on co-immobilization of both aptamer and co-adsorbent at the same. The proposed surface chemistry can be further studied and utilized for the development of a sensitive aptamer-based detection of MPT64 antigen.

#### 5. Acknowledgments

We would like to acknowledge Sunil K. Arya, Pavel Zhurauski and other members of the Biosensor Research Laboratory at the University of Bath for their help, advice and guidance. This work was supported by the British Council through a Newton-Al Farabi Fund researcher links travel grant (grant reference: 216423762).

#### Appendix

Supplementary Information.

601

602 **Author Contributions**

603     The manuscript was written through contributions of all authors. All authors have given ap-  
604     proval to the final version of the manuscript.

605

606

## References

- (WHO), W.H.O., 2016. Global Tuberculosis report. WHO Press.
- Aliakbarinodehi, N., Jolly, P., Bhalla, N., Miodek, A., De Micheli, G., Estrela, P., Carara, S., 2017. Aptamer-based field-effect biosensor for tenofovir detection. *Scientific Reports* 7, 44409.
- Andersen, P., Munk, M., Pollock, J., Doherty, T., 2000. Specific immune-based diagnosis of tuberculosis. *The Lancet* 356(9235), 1099-1104.
- Armbruster, D.A., Pry, T., 2008. Limit of Blank, Limit of Detection and Limit of Quantitation. *The Clinical Biochemist Reviews* 29(Suppl 1), S49-S52.
- Armbruster, D.A., Tillman, M.D., Hubbs, L.M., 1994. Limit of detection (LQD)/limit of quantitation (LOQ): comparison of the empirical and the statistical methods exemplified with GC-MS assays of abused drugs. *Clinical Chemistry* 40(7 Pt 1), 1233-1238.
- Arora, J., Kumar, G., Verma, A.K., Bhalla, M., Sarin, R., Myneedu, V.P., 2015. Utility of MPT64 Antigen Detection for Rapid Confirmation of Mycobacterium tuberculosis Complex. *Journal of Global Infectious Diseases* 7(2), 66-69.
- Asad-Ur-Rahman, F., Saif, M.W., 2016. Elevated level of serum carcinoembryonic antigen (CEA) and search for a malignancy: a case report. *Cureus* 8(6), e648.
- Bai, L.J., Chen, Y.H., Bai, Y., Chen, Y.J., Zhou, J., Huang, A.L., 2017. Fullerene-doped polyaniline as new redox nanoprobe and catalyst in electrochemical aptasensor for ultrasensitive detection of Mycobacterium tuberculosis MPT64 antigen in human serum. *Biomaterials* 133, 11-19.
- Balamurugan, S., Obubuafo, A., Soper, S.A., McCarley, R.L., Spivak, D.A., 2006. Designing highly specific biosensing surfaces using aptamer monolayers on gold. *Langmuir* 22(14), 6446-6453.
- Bekmurzayeva, A., Sypabekova, M., Kanayeva, D., 2013. Tuberculosis diagnosis using immunodominant, secreted antigens of Mycobacterium tuberculosis. *Tuberculosis* 93(4), 381-388.
- Benchimol, S., Fuks, A., Jothy, S., Beauchemin, N., Shirota, K., Stanners, C.P., 1989. Carcinoembryonic antigen, a human tumor marker, functions as an intercellular adhesion molecule. *Cell* 57(2), 327-334.
- Chu, T.P.J., Yuann, J.M.P., 2011. Expression, purification, and characterization of protective MPT64 antigen protein and identification of its multimers isolated from nontoxic Mycobacterium tuberculosis H37Ra. *Biotechnology and Applied Biochemistry* 58(3), 185-189.
- Doumas, B.T., Watson, W.A., Biggs, H.G., 1971. Albumin standards and the measurement of serum albumin with bromocresol green. *Clinica Chimica Acta* 31(1), 87-96.
- Formisano, N., Bhalla, N., Heeran, M., Reyes Martinez, J., Sarkar, A., Laabei, M., Jolly, P., Bowen, C.R., Taylor, J.T., Flitsch, S., Estrela, P., 2016. Inexpensive and fast pathogenic bacteria screening using field-effect transistors. *Biosensors and Bioelectronics* 85, 103-109.
- Formisano, N., Jolly, P., Bhalla, N., Cromhout, M., Flanagan, S.P., Fogel, R., Limson, J.L., Estrela, P., 2015. Optimisation of an electrochemical impedance spectroscopy aptasensor by exploiting quartz crystal microbalance with dissipation signals. *Sensors and Actuators B-Chemical* 220, 369-375.

647 Giri, P.K., Kruh, N.A., Dobos, K.M., Schorey, J.S., 2010. Proteomic analysis identifies highly  
648 antigenic proteins in exosomes from *M. tuberculosis*-infected and culture filtrate protein-treated  
649 macrophages. *Proteomics* 10(17), 3190-3202.

650 He, X.M., Carter, D.C., 1992. Atomic structure and chemistry of human serum albumin. *Nature*  
651 358(6383), 209.

652 Jayasena, S.D., 1999. Aptamers: An emerging class of molecules that rival antibodies in  
653 diagnostics. *Clinical Chemistry* 45(9), 1628-1650.

654 Jolly, P., Batistuti, M.R., Miodek, A., Zhurauski, P., Mulato, M., Lindsay, M.A., Estrela, P., 2016a.  
655 Highly sensitive dual mode electrochemical platform for microRNA detection. *Scientific Reports*  
656 6, 36719.

657 Jolly, P., Damborsky, P., Madaboosi, N., Soares, R.R.G., Chu, V., Conde, J.P., Katrlík, J., Estrela,  
658 P., 2016b. DNA aptamer-based sandwich microfluidic assays for dual quantification and multi-  
659 glycan profiling of cancer biomarkers. *Biosensors & Bioelectronics* 79, 313-319.

660 Jolly, P., Formisano, N., Tkac, J., Kasak, P., Frost, C.G., Estrela, P., 2015. Label-free impedimetric  
661 aptasensor with antifouling surface chemistry: A prostate specific antigen case study. *Sensors and*  
662 *Actuators B-Chemical* 209, 306-312.

663 Jolly, P., Miodek, A., Yang, D.K., Chen, L.C., Lloyd, M.D., Estrela, P., 2016c. Electro-Engineered  
664 Polymeric Films for the Development of Sensitive Aptasensors for Prostate Cancer Marker  
665 Detection. *Acs Sensors* 1(11), 1308-1314.

666 Keighley, S.D., Li, P., Estrela, P., Mighorato, P., 2008. Optimization of DNA immobilization on  
667 gold electrodes for label-free detection by electrochemical impedance spectroscopy. *Biosensors &*  
668 *Bioelectronics* 23(8), 1291-1297.

669 Kohli, R., Punia, R.S., Kaushik, R., Kundu, R., Mohan, H., 2014. Relative value of  
670 immunohistochemistry in detection of mycobacterial antigen in suspected cases of tuberculosis in  
671 tissue sections. *Indian Journal of Pathology and Microbiology* 57(4), 574-578.

672 Kruh-Garcia, N.A., Wolfe, L.M., Chaisson, L.H., Worodria, W.O., Nahid, P., Schorey, J.S., Davis,  
673 J.L., Dobos, K.M., 2014. Detection of *Mycobacterium tuberculosis* Peptides in the Exosomes of  
674 Patients with Active and Latent *M. tuberculosis* Infection Using MRM-MS. *Plos One* 9(7),  
675 e103811.

676 Kuwahara, M., 2014. Progress in Chemically Modified Nucleic Acid Aptamers. *Chemical Biology*  
677 *of Nucleic Acids: Fundamentals and Clinical Applications*, 243-270.

678 Liang, G., Li, T., Li, X., Liu, X., 2013. Electrochemical detection of the amino-substituted  
679 naphthalene compounds based on intercalative interaction with hairpin DNA by electrochemical  
680 impedance spectroscopy. *Biosensors and Bioelectronics* 48, 238-243.

681 Mehaffy, C., Dobos, K.M., Nahid, P., Kruh-Garcia, N.A., 2017. Second generation multiple  
682 reaction monitoring assays for enhanced detection of ultra-low abundance *Mycobacterium*  
683 *tuberculosis* peptides in human serum. *Clinical Proteomics* 14, 21.

684 Miodek, A., Regan, E.M., Bhalla, N., Hopkins, N.A.E., Goodchild, S.A., Estrela, P., 2015.  
685 Optimisation and Characterisation of Anti-Fouling Ternary SAM Layers for Impedance-Based  
686 Aptasensors. *Sensors* 15(10), 25015-25032.

687 Nogues, C., Leh, H., Lautru, J., Delelis, O., Buckle, M., 2012. Efficient Antifouling Surface for  
688 Quantitative Surface Plasmon Resonance Based Biosensor Analysis. *PLoS One* 7(9), e44287.



Pinhata, J.M.W., Cergole-Novella, M.C., Carmo, A.M.D., Silva, R., Ferrazoli, L., Sacchi, C.T., de Oliveira, R.S., 2015. Rapid detection of Mycobacterium tuberculosis complex by real-time PCR in sputum samples and its use in the routine diagnosis in a reference laboratory. *Journal of Medical Microbiology* 64, 1040-1045.

Qin, L., Zheng, R., Ma, Z., Feng, Y., Liu, Z., Yang, H., Wang, J., Jin, R., Lu, J., Ding, Y., Hu, Z., 2009. The selection and application of ssDNA aptamers against MPT64 protein in Mycobacterium tuberculosis. *Clinical Chemistry and Laboratory Medicine* 47(4), 405-411.

Serec, K., Babić, S.D., Podgornik, R., Tomić, S., 2016. Effect of magnesium ions on the structure of DNA thin films: an infrared spectroscopy study. *Nucleic Acids Research* 44(17), 8456-8464.

Steel, A.B., Herne, T.M., Tarlov, M.J., 1998. Electrochemical Quantitation of DNA Immobilized on Gold. *Analytical Chemistry* 70(22), 4670-4677.

Stenman, U.-H., Leinonen, J., Zhang, W.-M., Finne, P., 1999. Prostate-specific antigen. *Seminars in cancer biology*, pp. 83-93. Elsevier.

Sypabekova, M., Bekmurzayeva, A., Wang, R.H., Li, Y.B., Nogues, C., Kanayeva, D., 2017. Selection, characterization, and application of DNA aptamers for detection of Mycobacterium tuberculosis secreted protein MPT64. *Tuberculosis* 104, 70-78.

Tadele, A., Beyene, D., Hussein, J., Gemechu, T., Birhanu, A., Mustafa, T., Tsegaye, A., Aseffa, A., Sviland, L., 2014. Immunocytochemical detection of Mycobacterium Tuberculosis complex specific antigen, MPT64, improves diagnosis of tuberculous lymphadenitis and tuberculous pleuritis. *BMC Infectious Diseases* 14, 9.

Thakur, H., Kaur, N., Sabherwal, P., Sareen, D., Prabhakar, N., 2017a. Aptamer based voltammetric biosensor for the detection of Mycobacterium tuberculosis antigen MPT64. *Microchimica Acta* 184(7), 1915-1922.

Thakur, H., Kaur, N., Sareen, D., Prabhakar, N., 2017b. Electrochemical determination of M. tuberculosis antigen based on Poly (3,4-ethylenedioxythiophene) and functionalized carbon nanotubes hybrid platform. *Talanta* 171, 115-123.

Thompson, I.M., Pauler, D.K., Goodman, P.J., Tangen, C.M., Lucia, M.S., Parnes, H.L., Minasian, L.M., Ford, L.G., Lippman, S.M., Crawford, E.D., 2004. Prevalence of prostate cancer among men with a prostate-specific antigen level  $\leq$  4.0 ng per milliliter. *New England Journal of Medicine* 350(22), 2239-2246.

## Figure legends

**Fig. 1.** An aptasensor surface modification based on different chemistries applied onto the gold surface of an electrode; (a) short linker DNA aptamer/MCH; (b) long linker DNA aptamer/EG; (c) long linker DNA aptamer/MCH. Not to scale.

**Fig. 2.** Target MPT64 detection using BioFET. (a) A typical  $I_D/V_{GS}$  characteristic curve for an electrode before (solid line) and after (dashed line) MPT64 binding event based on long linker aptamer/MCH complex. (b)  $V_{GS}$  changes on the surface of the electrode upon incubation with different MPT64 concentrations in SELEX buffer based on short linker aptamer/MCH (1/100 ratio), long linker aptamer/EG (1/100 ratio) and long linker aptamer/MCH (1/100 ratio). All measurements were repeated on three different electrodes.

**Fig. 3.** (a) Aptamer molecule density distribution on the electrode surface vs. aptamer/MCH molar fraction in solution. The measurements were based on the resulting charge change in the absence and presence of 100  $\mu$ M hexaammineruthenium (III) chloride ( $\text{Ru}(\text{NH}_3)_6^{3+}$ ) in 10 mM Tris-HCl pH 7.4. (b) Change in charge transfer resistance ( $R_{ct}$ ) of an electrode measured in 30 min intervals at different MPT64 concentrations binding at different aptamer/MCH ratios. The measurements were recorded in SELEX buffer containing 2 mM ferro/ferricyanide  $[\text{Fe}(\text{CN})_6]^{3-/4-}$  redox couple. Error bars show the mean and spread for at least three measurements from different electrodes.

**Fig. 4.** (a) A schematic overview of the gold electrode surface modification with a long linker DNA aptamer/MCH followed by the target MPT64 capturing event on the functionalized surface of the gold electrode; (b) A representative Nyquist plot ( $-Z''$  vs.  $Z'$ ) for an electrode with a bare surface, immobilized with the long linker DNA aptamer/MCH before and after interaction with MPT64 for 30 min. Calculated fitted values to the equivalent circuit are presented as dashed lines. (c) A concentration dependent curve for different MPT64 concentrations using a long linker DNA aptamer/MCH at a ratio of 1/100 relative to blank measurements from the EIS signal measured in SELEX buffer; (d) a Nyquist plot for different MPT64 concentrations (in nM) using a long linker DNA aptamer/MCH in a ratio of 1/100 (experimentally obtained values are shown as dots; fitted values are shown as dashed lines); Inset (for b and d): Randles equivalent circuit, where  $R_s$  is the solution resistance,  $R_{ct}$  is the charge transfer resistance,  $CPE$  is the constant phase element, and  $W$

is the Warburg element. Error bars show the mean and spread for at least three measurements from different electrodes.

**Fig. 5.** Specificity study of the electrochemical aptasensor for the target MPT64 detection along with HSA, CEA, and PSA detection at different concentrations based on a long linker DNA aptamer/MCH surface chemistry at an optimized ratio of 1/100. Change in charge transfer resistance ( $R_{ct}$ ) of an electrode measured in 30 min intervals in SELEX buffer containing 2 mM ferro/ferricyanide  $[\text{Fe}(\text{CN})_6]^{3-/4-}$  redox couple. Error bars show the mean and spread for at least three measurements from different electrodes.

**Fig. 6.** (a) A representative Nyquist plot ( $-Z''$  vs.  $Z'$ ) for an electrode immobilized with a long linker DNA aptamer/MCH in a buffer and in the serum. (b) Change in the charge transfer resistance ( $R_{ct}$ ) of an electrode measured in 30 min intervals at different MPT64 concentrations 1/100 diluted serum samples using EIS. Measurements were recorded in SELEX measurement buffer containing 2 mM ferro/ferricyanide  $[\text{Fe}(\text{CN})_6]^{3-/4-}$  redox couple. Black squares represent values obtained from incubation with different MPT64 concentrations diluted in serum. Dashed trend line represents repetitive measurements of serum sample without MPT64. Error bars show the mean and spread for at least three measurements from different electrodes.

772 **Table titles**

773

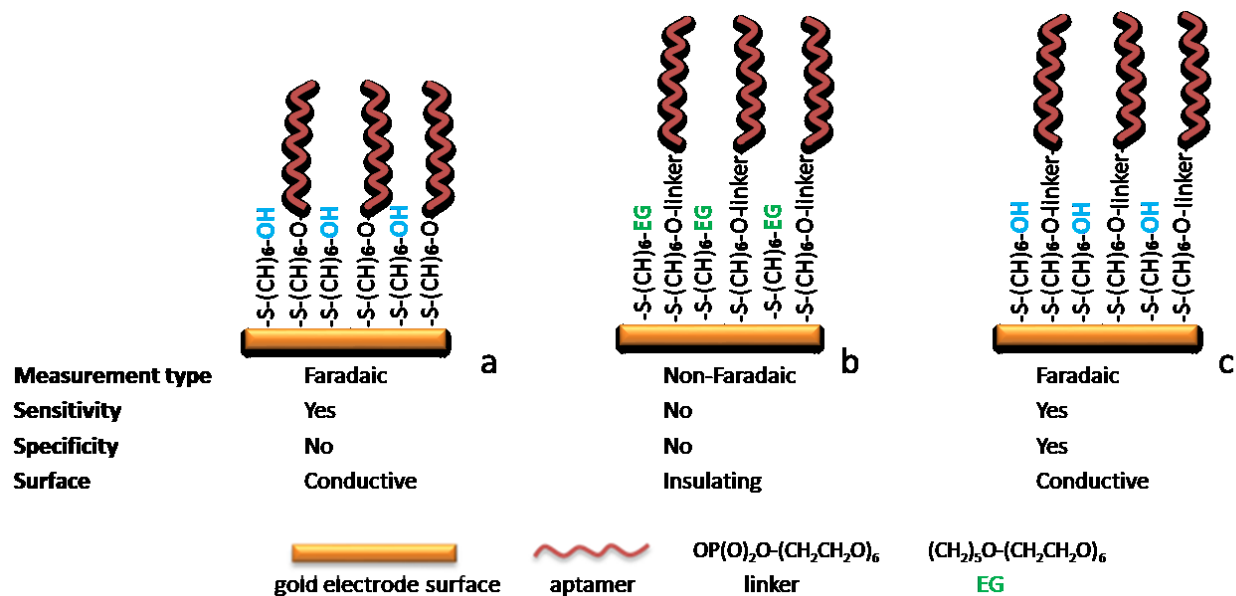
774 **Table 1.** Overview of TB detection methods described in the literature.

775

776 **Table 2.** Aptamer molecule density distribution on the electrode surface vs. aptamer/MCH molar  
777 fraction in solution.

778  
779

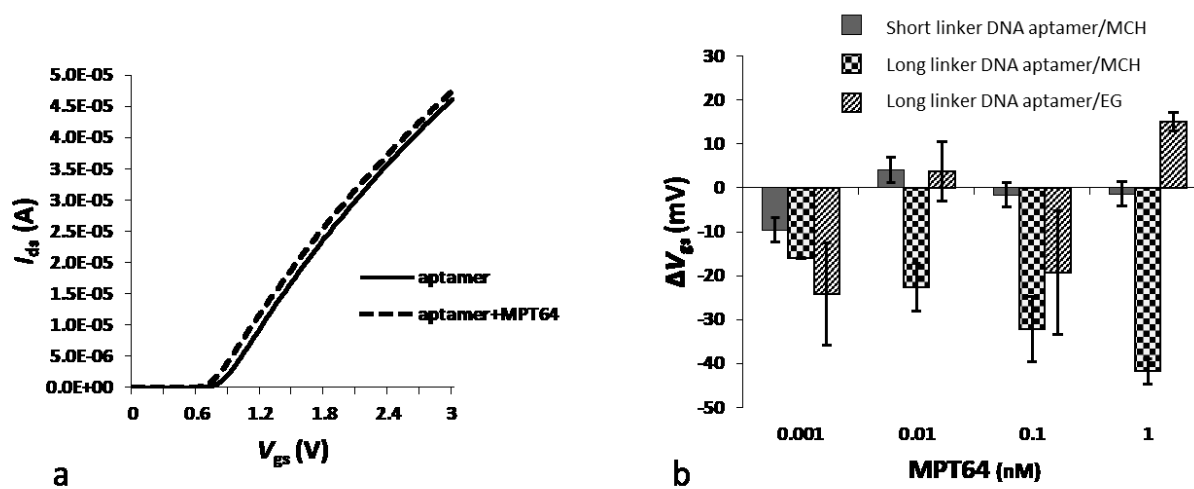
Fig. 1.



780  
781  
782

783  
784  
785

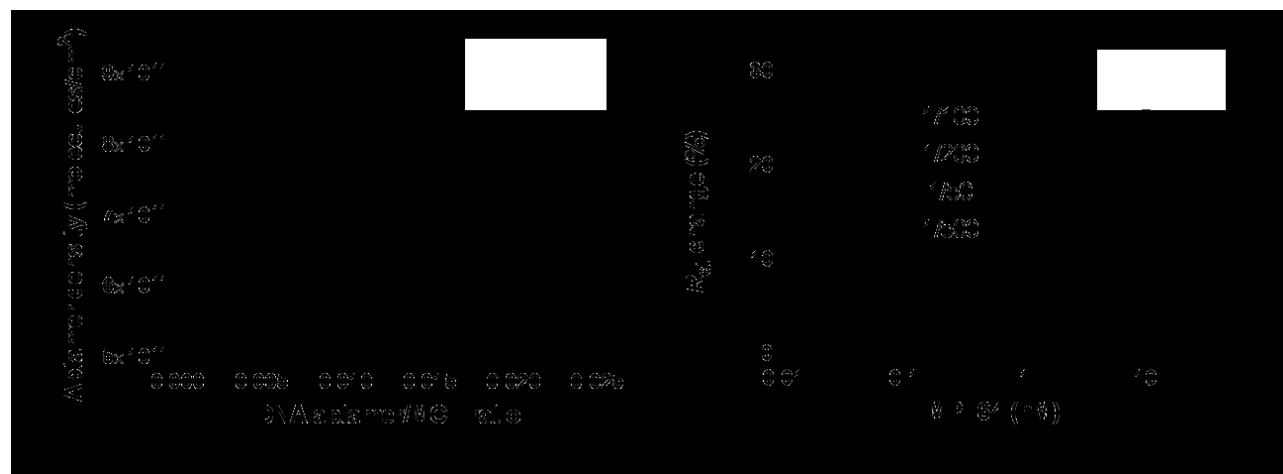
Fig. 2.



786

787  
788

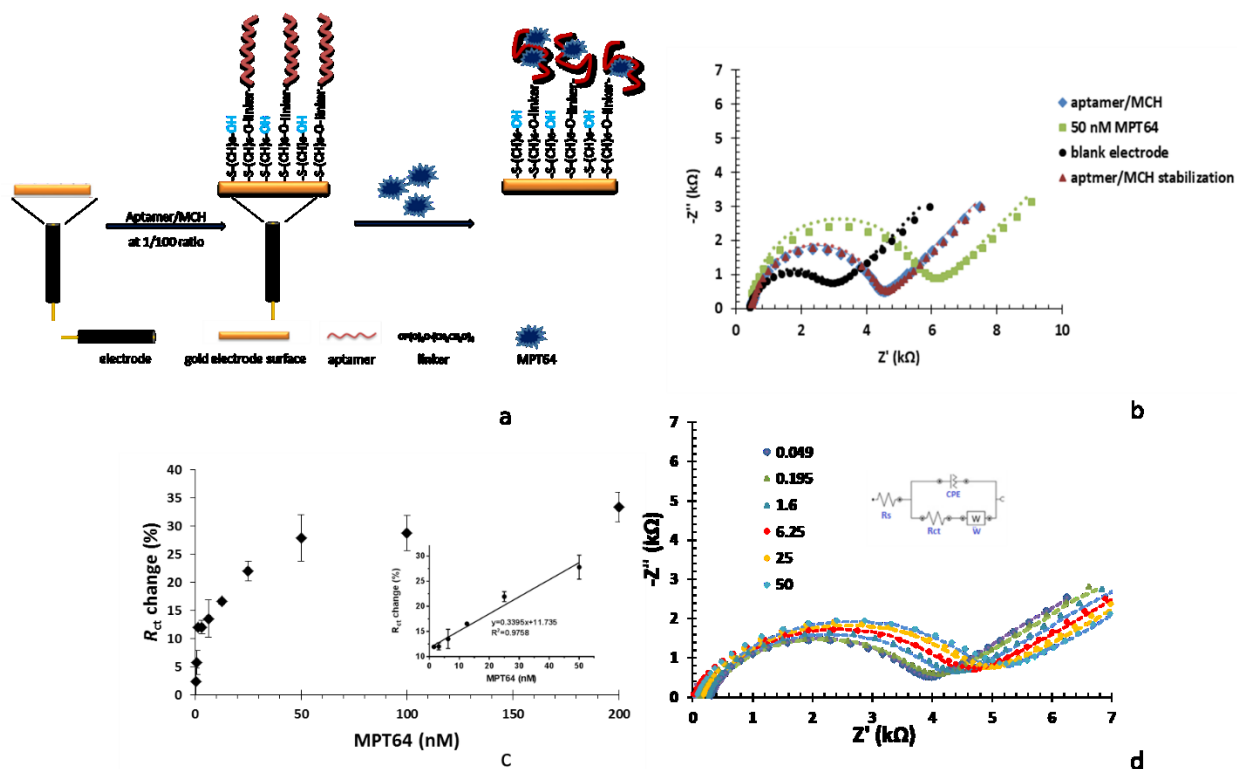
Fig. 3.



789  
790  
791  
792  
793

794  
795

Fig. 4.

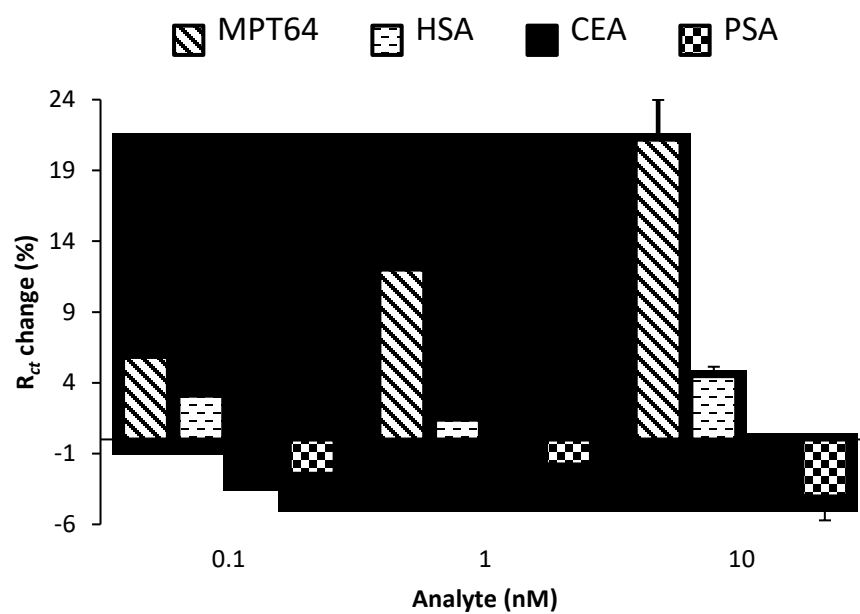


796  
797  
798



799  
800

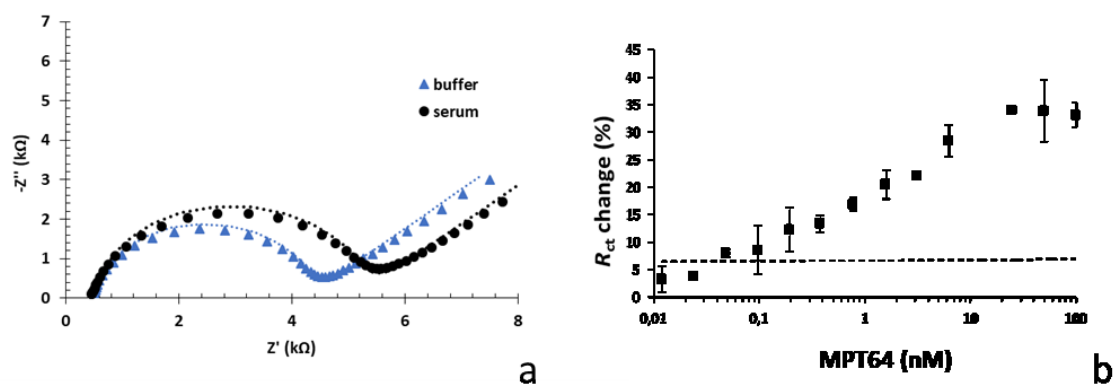
Fig. 5.



801  
802  
803

804  
805

Fig. 6.



806  
807

Type of method	Sub-division of type of method	Type of technique	Recognition molecule	Disadvantage	Advantage	Reference
Smear microscopy *	Acid-fast bacilli smear microscopy	Sputum smear microscopy	Cell staining	Low sensitivity, not specific to <i>Mtb</i>	Good in poor resource settings	(Parsons et al., 2011)
Culture method *	Automated	Bactec MGIT 960	Bacterial growth	Sophisticated instrument, contamination, disposal of radioactive material	Decrease in numbers of false positive results	(Tortoli et al., 1999)
	Automated	Mb/Bact system	Bacterial growth	Sophisticated instrument, contamination, disposal of radioactive material	Decrease in numbers of false positive results	(Díaz-Infantes et al., 2000)
	Automated	Esp culture system	Bacterial growth	Sophisticated instrument, contamination, disposal of radioactive material	Decrease in numbers of false positive results	(Bergmann and Woods, 1998)
	Semi-automated	Bactec 460	Bacterial growth	Sophisticated instrument, contamination, disposal of radioactive material	Decrease in numbers of false positive results	(Aggarwal et al., 2008)
Blood sample analysis based method	Bacterial detection	Bactec Myco/F Lytic Blood Culture	Bacterial growth	Sophisticated instrument, contamination, disposal of radioactive material	Decrease in numbers of false positive results	(Waite and Woods, 1998)
	Mediated interferon gamma (IFNg) detection	T-SPOTTB test	Antibody	No discrimination of latent TB from active	Response to multiple antigens and discrimination between <i>Mtb</i> and environmental mycobacteria	(Herrera et al., 2011; Pai et al., 2014; Richeldi, 2006)
	Mediated interferon gamma (IFNg) detection	QuantiFeron TB	Antibody	No discrimination of latent TB from active	Response to multiple antigens and discrimination between <i>Mtb</i> and environmental mycobacteria	(Sultan et al., 2013)

Molecular method	Nucleic acid amplification test (PCR, RT-PCR)	Amplification of TB signature genes	DNA hybridization	Sophisticated instrument and expensive reagents	Information of size and sequence of a gene and drug resistance can be obtained	(Kiraz et al., 2010; Russo et al., 2006; Sambarey et al., 2017; Sharma et al., 2012;)
		Xpert MTB/RIF assay *	DNA hybridization	Sophisticated instrument and expensive reagents	Information of size and sequence of a gene and drug resistance can be obtained	(Marlowe et al., 2011)
		Genotype MTBDR plus	DNA hybridization	Sophisticated instrument and expensive reagents	Information of size and sequence of a gene and drug resistance can be obtained	(Hillemann et al., 2007)
		DNA hybridization (microarrays)	DNA hybridization	Sophisticated instrument and expensive reagents	Information of size and sequence of a gene and drug resistance can be obtained	(Talaat et al., 2002)
	DNA sequencing	Whole genome sequencing	DNA hybridization	Sophisticated instrument and expensive reagents	Information of size and sequence of a gene and drug resistance can be obtained	(Lee and Behr, 2016; Walker et al., 2015)
		Specific gene sequencing	DNA hybridization	Sophisticated instrument and expensive reagents	Information of size and sequence of a gene and drug resistance can be obtained	(Zhang et al., 2013)
Skin patch	Tuberculin skin test (TST)		Antibody	Follow-up visit required; wide range of sensitivities and specificities	No sample preparation/treatment required	(Chaudhary et al., 2010)
Immune-based method	Immunochromatographic	One-Step TB Test Kit; Tell Me Fast <i>MTB</i> IgG/IgM Test Device; Capilia TB; SD Bioline TB AG Mpt64; SD TB IgG/IgM; BD MGIT	Antibody	No discrimination between MTB species	Mutation or deletion of the target gene can result in false negatives	(Ngeow et al., 2011; Shen et al., 2011; Toiher et al., 2011)

Electro-chemical detection	Differential pulse voltammetry (DPV)	Electropolymerised Poly(3,4-ethylenedioxythiophene) doped with carbon nanotubes	aptamer 77 nucleotides	Relatively complex surface chemistry. The sensor needs to be validated in real TB samples.	Detection limit within clinical detection range	(Thakur et al., 2017b)
	DPV	Sandwich scheme based on: gold nanoparticles decorated with fullerene-doped polyaniline	aptamer 35 nucleotides	Relatively complex surface chemistry. The sensor needs to be validated in real TB samples.	Detection limit within clinical detection range	(Bai et al., 2017)
	DPV	Graphene modified iron-oxide chitosan hybrid nanocomposite film deposited on fluorine tin oxide	aptamer 77 nucleotides	Relatively complex surface chemistry. The sensor needs to be validated in real TB samples.	Detection limit within clinical detection range	(Thakur et al., 2017a)
	EIS	IDM bare gold electrode with MCH as co-adsorbent	aptamer 40 nucleotides	The sensor needs to be validated with real TB samples	Simple surface chemistry, detection limit within clinical detection range	This work

---

\* - routinely used assays in anti-tuberculosis dispensaries approved by WHO.

814  
815  
816

Table 2

Aptamer/MCH ratio	Mean of measurements from three electrodes (mole- cules/cm <sup>2</sup> )
1/50 (0.002%)	6.50×10 <sup>11</sup>
1/100 (0.005%)	7.34 x 10 <sup>11</sup>
1/200 (0.01%)	7.66 x 10 <sup>11</sup>
1/500 (0.02%)	7.91×10 <sup>11</sup>

817